

## Polarized electroabsorption spectroscopy of highly ordered poly(2-methoxy,5-(2'-ethyl-hexoxy)-*p*-phenylene vinylene)

T. W. Hagler

*Los Alamos National Laboratory, Los Alamos, New Mexico 87545*

K. Pakbaz and A. J. Heeger

*Department of Physics and Institute for Polymers and Organic Solids, University of California, Santa Barbara, Santa Barbara, California 93106*

(Received 6 September 1994)

We present a quantitative analysis of the absorption and field-induced absorption (electroabsorption) spectra of dilute blends of the conjugated polymer poly[2-methoxy,5-(2'-ethyl-hexoxy)-*p*-phenylene vinylene] (MEH-PPV) oriented in ultrahigh molecular weight polyethylene (PE). Because of the orientation, the enhanced order and the dilution of the MEH-PPV conjugated polymer in the polyethylene matrix, the MEH-PPV/PE blend is an ideal system in which to investigate the intrinsic linear and nonlinear optical properties of oriented conjugated polymer chains; the absorption is directly proportional to the imaginary part of  $\chi^{(1)}(\omega)$  and the electroabsorption is directly proportional to the imaginary part of  $\chi^{(3)}(\omega, 0, 0)$  of the oriented, ordered MEH-PPV  $\pi$ -electron system. The optical data obtained from the oriented blends are, therefore, directly relevant to theoretical models which describe the intrinsic electronic structure of the conjugated polymer; i.e., models which do not account for disorder. Using a model based on the continuum version of the Su-Schrieffer-Heeger theory, we simultaneously fit to the absorption and electroabsorption spectra, and demonstrate that the intrinsic optical line shape of MEH-PPV oriented in polyethylene is highly asymmetric, and can be modeled accurately in terms of a Gaussian-broadened one-dimensional square-root singularity in the joint density of states.

### I. INTRODUCTION

Although the linear and nonlinear optical properties of conjugated polymers have been investigated for over a decade, there is still controversy over the description of the elementary excitations in these systems. The central issue is the relative strengths of the electron-electron and the electron-phonon interactions in comparison with the  $\pi$ -electron bandwidth. For systems dominated by the Coulomb interaction, momentum conservation in the center-of-mass coordinate requires that only the zero-momentum excitons couple to the optical field.<sup>1</sup> As the exciton binding energy is increased, oscillator strength is transferred from the continuum and higher lying bound exciton states to the lowest discrete exciton state, and in the limit of large Coulomb binding energy, there becomes only one dominant dipole allowed transition from the ground state (i.e., to the  $^1B_u$  exciton).<sup>2</sup> As a consequence, the absorption and electroabsorption line shapes will appear symmetric. In contrast, an interband transition is expected to yield an asymmetric line shape in a quasi-one-dimensional system, which reflects the square-root singularity in the joint density of states.<sup>3</sup> Therefore, an accurate analysis of the linear and nonlinear susceptibility line shapes should provide some insight into the relative importance of the exciton binding energy in conjugated polymers.

When analyzing the optical spectra of a given con-

jugated polymer sample, one must consider the effects of disorder on the measured line shape. Tokihiro and Hanamura<sup>4</sup> demonstrated that random disorder can lead to a violation of momentum conservation, which can yield an asymmetric line shape even in the Frenkel exciton limit. Another type of disorder involves samples with a distribution of conjugation lengths. Bäessler and co-workers, citing the results of site-selective fluorescence measurements,<sup>5-7</sup> and the first-derivative nature of the electroabsorption line shape,<sup>8,9</sup> have concluded that the elementary excitations in PPV and its derivatives are highly localized Frenkel/Wannier excitons residing on finite conjugated segments delineated by disorder. In this case, the observed absorption line shape is derived from a superposition of finite conjugated segments. Since the energy eigenstates are assumed to be tightly bound excitons, the absorption line shapes of the individual conjugated segments are inherently symmetric; the measured asymmetry simply reflects the segment distribution function and the conjugation length dependence of the  $\pi - \pi^*$  energy gap.

In order to investigate the *intrinsic* optical properties of the quasi-one-dimensional electronic system, it is essential to have conjugated polymer samples of sufficient order that the optical properties of the material are not dominated by the conjugation length distribution function or random disorder. In a previous study, Hagler *et al.*<sup>10</sup> demonstrated that the structural order of 2-

methoxy,5-(2-ethyl-hexoxy)-*p*-phenylene vinylene (MEH-PPV) could be significantly enhanced by fabricating oriented, dilute blends of the conjugated polymer in ultrahigh molecular weight polyethylene, MEH-PPV/PE. When compared to cast films of the pure polymer MEH-PPV, the oriented blends displayed a sharpening of the vibronic structure and a redistribution of spectral weight into the zero-phonon line, in both absorption and emission, for light polarized parallel to the draw axis. The induced order was sufficient to demonstrate that the intrinsic line shape of the absorption was highly asymmetric, and could be modeled accurately in terms of a Gaussian-broadened square-root singularity in the joint density of states.

In addition to the enhanced quality of the absorption and emission spectra, the polarized electroabsorption and photoluminescence spectra of tensile drawn MEH-PPV/PE are both strongly anisotropic, with polarization ratios in excess of 150:1 and 60:1, respectively.<sup>10,11</sup> Using a model for the off-axis transition dipole moment of the conjugated polymer, which is based on the measured off-axis transition dipole moment of *trans*-stilbene<sup>12</sup> and the geometric structure of MEH-PPV, it was shown that the polarization anisotropy of the field-induced absorption requires that the instantaneous excited state wave functions in structurally ordered MEH-PPV are delocalized over a minimum of 50 unit cells. The combined analysis of the polarized absorption, photoluminescence, and electroabsorption spectra in the oriented MEH-PPV/PE blends indicate that the intrinsic energy eigenstates are highly delocalized, and that the joint density of states is unambiguously asymmetric. Since the spatial extent of the instantaneous excited state wave functions encompasses some 400  $\pi$  electrons, it seems reasonable to suggest that the asymmetric line shape of the oriented MEH-PPV/PE blend is the characteristic signature of a one-dimensional band structure.

In this paper, we present an analysis of the intrinsic line shape of the polarized absorption and field-induced absorption (electroabsorption) spectra of the conjugated polymer MEH-PPV oriented in polyethylene. Using a model,<sup>13</sup> which is based on the continuum version of the Su-Schrieffer-Heeger (SSH) formalism,<sup>14–16</sup> we fit to both the absorption and electroabsorption spectra, and demonstrate that the intrinsic optical line shape of structurally ordered MEH-PPV in polyethylene is highly asymmetric, and can be modeled accurately in terms of a Gaussian-broadened one-dimensional square-root singularity in the joint density of states. By comparing the absorption and electroabsorption fitting parameters, we demonstrate that both the linear and nonlinear optical response of the oriented blend can be accurately described in terms of the SSH theory with a limited number of parameters, and that these properties are not dominated by disorder or a distribution of conjugation lengths.

## II. ANALYSIS OF THE ABSORPTION AND ELECTROABSORPTION LINE SHAPES

### A. Time-dependent perturbation theory

The third-order process responsible for field-induced absorption is a special case of the more general four-wave

mixing phenomena,  $\chi^{(3)}(\omega_4 : \omega_1, \omega_2, \omega_3)$ , where two of the fields are applied with vanishing frequency.<sup>17</sup> Hence, the transition dipole moment matrix elements, which determine the sequence of virtual transitions responsible for the quadratic field-induced absorption, are the same for all third-order nonlinear optical phenomena.<sup>17</sup> The instantaneous processes responsible for electric field modulation (EFM) are identical to those responsible for electric-field-induced second harmonic, two-photon absorption, and third harmonic generation, only they are weighted by different resonant denominators. The generic virtual third-order sequence describing these third-order processes is given by

$$\langle g|\mathbf{r}|l\rangle\langle l|\mathbf{r}|m\rangle\langle m|\mathbf{r}|n\rangle\langle n|\mathbf{r}|g\rangle, \quad (1)$$

where  $|g\rangle$  is the many-body ground state of the unperturbed Hamiltonian. The only requirements on  $|l\rangle$ ,  $|m\rangle$ , and  $|n\rangle$  are that they are eigenstates of the unperturbed many-body Hamiltonian as well. In conjugated polymers, which are members of the  $C_{2h}$  point group, symmetry considerations specify that  $|l\rangle$  and  $|n\rangle$  are of  $B_u$  symmetry and  $|g\rangle$  and  $|m\rangle$  are of  $A_g$  symmetry.

### B. Relevant intermediate states: Exciton or band description?

Recently, the absence of a third-derivative or Franz-Keldysh line shape<sup>18–20</sup> in the electroabsorption spectra of PPV and its derivatives has been cited as “conclusive evidence” that the elementary excitations in conjugated polymers are tightly bound excitons.<sup>8,9</sup> While the first-derivative line shape is the general perturbation theory result,<sup>17</sup> the third-derivative or Franz-Keldysh line shape requires the existence of an intraband contribution to the third-order nonlinear susceptibility.<sup>20</sup> Therefore, while the lack of a third-derivative or Franz-Keldysh line shape to the EFM spectrum does imply the relative unimportance of intraband processes to the nonlinear susceptibility in conjugated polymers, it does not constitute evidence for a large Coulomb binding energy, nor does it invalidate a band structure description of the first optically allowed transition. This is clearly demonstrated in electroabsorption studies on amorphous inorganic semiconductors, where in contrast to the crystalline state, the amorphous materials show no evidence of a third-derivative or Franz-Keldysh line shape in the electroabsorption spectra.<sup>21–25</sup> In fact, if one ignores the obviously different electron-phonon interaction, the amorphous inorganic semiconductors demonstrate field-induced absorption line shape characteristics, which are very similar to those observed in amorphous organic semiconductors such as PPV.

The origin of the field-induced absorption signal in amorphous inorganic semiconductors has also been the subject of considerable debate. Proposed mechanisms have included a disordered Franz-Keldysh effect,<sup>26–28</sup> a broadening of disordered exciton states,<sup>21</sup> and transitions between localized and extended states.<sup>22</sup> Several authors have cited the polarization anisotropy of the field-induced absorption in amorphous inorganic semiconductors as an insurmountable obstacle to these descriptions, and have argued in favor of models which are based on energy

dependent<sup>23–25</sup> or field-dependent transition dipole moment matrix elements.<sup>29</sup>

Objections to the more conventional field-induced absorption mechanisms, which are based on polarization dependent electroabsorption measurements are open to debate in light of a recent paper by Hagler,<sup>30</sup> who demonstrated that the polarization anisotropy of the field-induced absorption in isotropic media is a simple consequence of the tensor nature of the third-order nonlinear refractive index. The polarization anisotropy is a function of the relative angle between the dominant transition dipole moments responsible for the field-induced absorption, and has a maximum value of 3:1 for parallel transition dipole moments and a minimum value of 1:3 for perpendicular transition dipole moments. Since the field-induced absorption polarization anisotropy of all amorphous semiconductors fall within this range, the validity of the modified Franz-Keldysh or disordered exciton descriptions must be reexamined.

### C. A modified Franz-Keldysh description of electroabsorption in MEH-PPV

Because of the observed square-root singularity in the optical absorption line shape and the first-derivative nature of the field-induced absorption line shape, we consider a modified Franz-Keldysh description of the field-induced absorption in MEH-PPV in which  $\chi^{(3)}(\omega, 0, 0)$  is dominated by matrix elements involving a single even parity state, which we designate the dominant  ${}^m A_g$  symmetry state. The intraband contribution is assumed to be quenched by the finite coherence length of the excited state wave function,<sup>20,26–28</sup> an effect which has been experimentally verified in electroabsorption studies on polydiacetylene samples with varying degrees of order.<sup>31</sup>

The  $B_u$  symmetry states are taken to be the usual SSH extended band states,<sup>3</sup> which satisfy the following optical transition energy dispersion relation in the continuum limit,<sup>14–16</sup>

$$E_{cv}(k) = 2\Delta_0 \sqrt{(k\xi_k)^2 + 1} + i\Gamma_k/2, \quad (2)$$

where  $2\Delta_0$  is the energy gap,  $\xi_k$  is the linearization parameter, and  $\Gamma_k$  is the inverse autocorrelation time of the excited state.

Since the excited state wave function was previously demonstrated to extend over several unit cells,<sup>11</sup> we chose to model the dominant  ${}^m A_g$  symmetry state in the two-particle effective mass approximation,<sup>13</sup>

$$|{}^m A_g\rangle = \sum_k \sum_q |\psi_k^i \psi_q^j\rangle \langle \psi_k^i \psi_q^j | {}^m A_g\rangle \quad (i, j = v, c), \quad (3)$$

where the independent sum over  $k$  and  $q$  results from the two-particle nature of the  ${}^m A_g$  symmetry state, as required by charge conjugation symmetry.

The expansion coefficients  $\langle \psi_k^i \psi_q^j | {}^m A_g\rangle$  project the wave function of the  ${}^m A_g$  symmetry state onto the valence and conduction band continuum. Hence, the dipole moment matrix element between the  ${}^m A_g$  states and the

delocalized  ${}^k B_u$  states is weighted by the expansion coefficients  $\langle \psi_k^i \psi_q^j | {}^m A_g\rangle$ ; the linear absorption measures the projection of the  ${}^k B_u$  manifold onto the ground state, while the field-induced absorption measures the projection of the  ${}^k B_u$  manifold onto both the ground state and the  ${}^m A_g$  manifold. As a result, the optical line shape of the  ${}^k B_u$  states in the third-order process is modified (spectrally filtered) by coupling to the  ${}^m A_g$  states. A simple Fourier analysis reveals that if the  ${}^m A_g$  state is delocalized, the transition dipole moment couples more strongly to states near the  ${}^k B_u$  band edge. Conversely, if the  ${}^m A_g$  state is localized, the transition dipole moment is more uniform in the Bloch wave vector  $k$ . Hence, by comparing the  ${}^k B_u$  optical line shape derived from the absorption spectrum with that derived from the EFM spectrum, the localization length of the  ${}^m A_g$  state can, in principle, be deduced.

### D. Fitting procedure

In general, the field-induced absorption spectrum must be fit by a two step process: First, the parameters of the linear optical susceptibility must be fit to the absorption spectra. Then, using the derived linear optical functions,  $n_0(\omega)$  and  $\kappa_0(\omega)$ , the parameters for the nonlinear optical susceptibility must be fit to the experimentally measured quantity  $-\Delta T/T$ . A significant reduction in complexity is encountered when modeling the absorption and the electroabsorption in the MEH-PPV/PE blend; because of the dilution of the MEH-PPV within the polyethylene matrix, the absorption is directly proportional to the imaginary part of  $\chi^{(1)}(\omega)$  and  $-\Delta T/T$  is directly proportional to the imaginary part of  $\chi^{(3)}(\omega, 0, 0)$  of the oriented, ordered MEH-PPV  $\pi$ -electron system.

#### 1. Disorder and spectrometer resolution

The linear and nonlinear susceptibility are assumed to be that derived for a one-dimensional semiconductor with a simple vibronic interaction in the context of the Su-Schrieffer-Heeger (SSH) theory,<sup>3</sup> but assuming a Gaussian distribution of the energy gap (to account for disorder) centered about the mean value,  $2\Delta_0$ . The total line shape broadening is given by the convolution of the disorder  $\gamma_0$  and the wavelength-dependent resolution of the spectrometer  $\gamma_\lambda$ :

$$\chi^{(n)}(\omega) = \frac{1}{\sqrt{2\pi(\gamma_0^2 + \gamma_\lambda^2)}} \times \int d\Delta \exp\left\{-\frac{(\Delta - \Delta_0)^2}{\gamma_0^2 + \gamma_\lambda^2}\right\} \chi^{(n)}(\omega; \Delta, \eta), \quad (4)$$

where  $\chi^{(n)}(\omega)$  is the  $n$ th order susceptibility, and  $\eta$  is the fitting parameter vector. For the absorption and electroabsorption spectra shown in Ref. 10 and Ref. 11, respectively, the resolution of the spectrometer was chosen to be 1.6 nm and 5.2 nm, respectively.

## 2. Linear susceptibility model

The energy-gap dependent linear susceptibility functions are given by<sup>13,17</sup>

$$\chi^{(1)}(\omega; \Delta, \eta) = c_{b_u}^{(1)} \sum_{k, \nu} \frac{f_{cv}^2(k)}{[E_{cv}(k) + \nu \hbar \omega_{ph} - \omega]} \times \left[ \frac{e^{-S} S^\nu}{\nu!} \right] \quad (5)$$

where  $f_{cv}(k)$  is the SSH dipole moment matrix element,<sup>3</sup> and  $S$  and  $\nu$  are the Huang-Rhys parameter and vibronic index associated with the  $G$  to  ${}^k B_u$  electronic transition.<sup>32</sup> The following nonlinear fitting parameters were used in the linear absorption fitting routine:

$$\eta = \Delta_0, \Gamma_k, \gamma_0, S, \omega_{ph}. \quad (6)$$

## 3. Nonlinear susceptibility model

The total electroabsorption line shape was broken up into four terms which differ by the structural form of the resonant denominators.<sup>17</sup> Each of these terms is written as a sum of vibronic components weighted by the appropriate Franck-Condon vibronic overlap factor.<sup>32</sup>

After our initial attempts to fit the MEH-PPV/PE electroabsorption spectrum, it became apparent that the line shape could be modeled rather accurately with the following much simplified form for the third-order nonlinear susceptibility:

$$\chi^{(3)}(\omega, 0, 0; \Delta, \eta) = c_{b_u}^{(3)} \sum_{\nu} L_{b_u}^{(3)}(\omega; \Delta, \eta) \left[ \frac{e^{-S} S^\nu}{\nu!} \right]^2 + c_{a_g}^{(3)} L_{a_g}^{(3)}(\omega; \Delta, \eta), \quad (7)$$

where  $L_{b_u}^{(3)}$  is the third-order line shape function, which yields the first-derivative contribution to the field-induced absorption line shape,

$$L_{b_u}^{(3)}(\omega; \Delta, \eta) = \left( \sum_k \frac{f_{cv}(k) f_{cm}(k)}{[E_{cv}(k) + \nu \hbar \omega_{ph} - \omega]} \right)^2 \frac{1}{E_m}, \quad (8)$$

and  $L_{a_g}^{(3)}$  is the third-order line shape function, which contains the  ${}^m A_g$  state resonance,

$$L_{a_g}^{(3)}(\omega; \Delta, \eta) = \left( \sum_k \frac{f_{cv}(k) f_{cm'}(k)}{E_{cv}(k)} \right)^2 \frac{1}{(E_m + i\Gamma_m - \omega)}, \quad (9)$$

where  $E_m$  and  $\Gamma_m$  are the energy and linewidth of the  ${}^m A_g$  state, respectively.

The dipole moment matrix elements between the  ${}^k B_u$  states and the  ${}^m A_g$  symmetry state are treated in the effective mass approximation as follows:<sup>13</sup>

$$f_{cm}(k) = \langle {}^m A_g | y | {}^k B_u \rangle = f_{cm}^0 \operatorname{sech}^2 \left( \frac{\pi}{2} k \xi_m \right) \left| \frac{2\Delta}{E_{cv}(k)} \right|. \quad (10)$$

In the effective mass picture, the dipole moment matrix elements  $\langle {}^m A_g | y | {}^k B_u \rangle$  are a strong function of the  ${}^m A_g$  state localization length,  $\xi_m$ , and hence, the analysis of the EFM spectra provides us with information of the localization length of the  ${}^m A_g$  state.

The following nonlinear fitting parameters were used in the field-induced absorption fitting routine:

$$\eta = \Delta_0, \Gamma_k, \gamma_0, S, \omega_{ph}, \xi_m, E_m, \Gamma_m. \quad (11)$$

## III. RESULTS OF THE FITTING PROCEDURE

### A. Linear susceptibility

Figure 1 shows the results of the 80 K absorption fitting routine. The open circles are the data and the solid line is the fit corresponding to the parameters listed in Table I. To determine the quality of the fit,  $\chi^2$  was set equal to one, and we solved for the standard deviation in the data set,  $\Delta y$ . From the fit, we find  $\Delta y \approx 1.7\%$ , which is approximately the rated stability of our lamp power supply. The discrepancy between the data and the fit below 2.1 eV is due to residual scattering of the polyethylene matrix.<sup>10</sup>

In Fig. 2 we show the first derivative of the 80 K absorption spectrum (dashed line) and the first derivative of the fit shown in Fig. 1 (solid line). The figure demonstrates that the actual absorption onset is more abrupt than the one calculated from the model. This is probably due to the fact that the Gaussian distribution does not reflect the saturation of the energy gap in the long chain limit. Note the general agreement with the position and

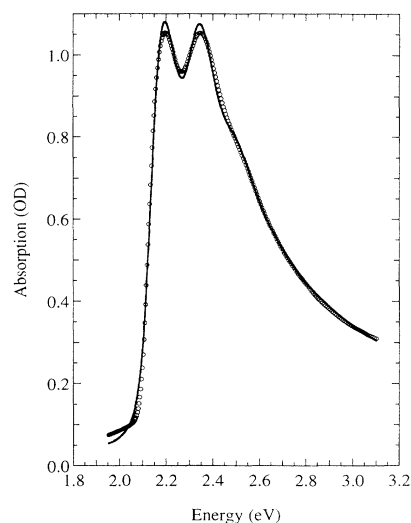


FIG. 1. The results of the 80 K absorption fitting routine. The open circles are the data and the solid line is the fit corresponding to the parameters listed in Table I. To determine the quality of the fit,  $\chi^2$  was set equal to one and we solved for the standard deviation in the data set,  $\Delta y$ . We found  $\Delta y \approx 1.7\%$ , which is approximately the rated stability of our lamp power supply.

TABLE I. Analysis of  $B_u$  symmetry states in MEH-PPV/PE.

| Exp. | $2\Delta_0$ (eV) | $\Gamma_k$ (eV) | $\gamma_0$ (eV) | $\hbar\omega_{ph}$ (eV) | $S$  | $\Delta y$ |
|------|------------------|-----------------|-----------------|-------------------------|------|------------|
| EFM  | 2.141            | 0.03            | 0.03            | 0.185                   | 0.44 | 0.029      |
| ABS  | 2.145            | 0.04            | 0.04            | 0.167                   | 0.45 | 0.017      |

overall width of the vibronic structure.

The optical absorption line shape demonstrates energy dispersion which is accurately modeled in terms of a Gaussian-broadened one-dimensional square-root singularity in the joint density of states. The absorption line shape cannot be modeled in terms of a single Franck-Condon progression of Lorentzian, Gaussian or Gaussian broadened Lorentzian line shapes. This is clearly indicated by the Huang-Rhys parameter, which is identical to that determined from the corrected photoluminescence spectrum.<sup>10</sup> If the *intrinsic* line shape of the MEH-PPV/PE blend was more symmetric than the assumed Gaussian broadened square-root singularity, the Huang-Rhys parameter required to fit the absorption spectrum would be substantially larger than that found for the photoluminescence spectrum,<sup>10</sup> which is inconsistent with energy conservation.

### B. Nonlinear susceptibility

In Fig. 3, we present the results of the 80 K electroabsorption fitting routine. The open circles are the data and the solid line is the fit corresponding to the parameters listed in Table I. To determine the quality of the fit,  $\chi^2$  was set equal to one and we solved for the standard deviation in the data set,  $\Delta y$ . From the fit, we find

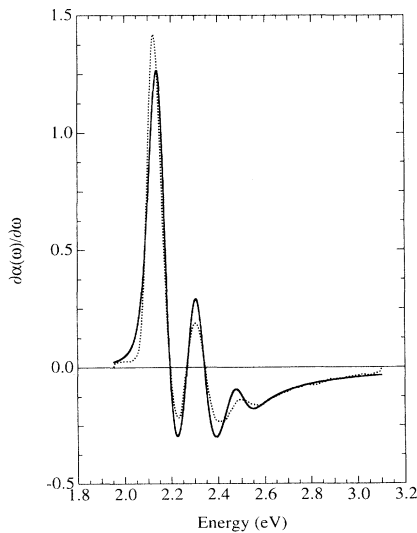


FIG. 2. The first derivative of the 80 K absorption spectrum (dashed line) and the first derivative of the fit (solid line). The figure demonstrates that the actual absorption onset is sharper than the one calculated from the model.

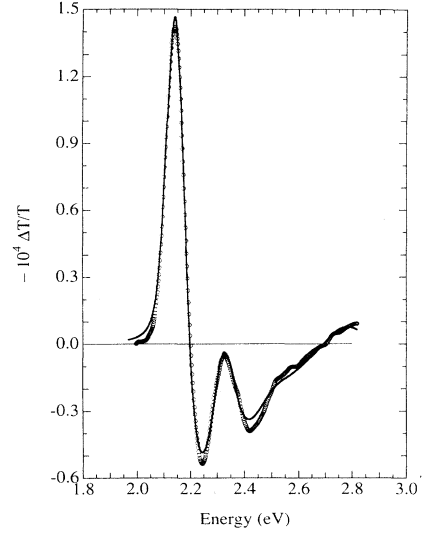


FIG. 3. The results of the 80 K electroabsorption fitting routine. The open circles are the data and the solid line is the fit corresponding to the parameters listed in Table I. To determine the quality of the fit,  $\chi^2$  was set equal to one and we solved for the standard deviation in the data set,  $\Delta y$ . We found  $\Delta y \approx 2.9\%$ , a value consistent with the noise level of our electroabsorption apparatus. The figure demonstrates that the actual field-induced absorption onset is sharper than the one calculated from the model. The shoulder appearing in the data at 2.35 eV is likely vibronic in origin.

$\Delta y \approx 2.9\%$ , a value consistent with the noise level of our electroabsorption apparatus; approximately  $2 \mu\text{V}$  at 4 kV applied bias. The deviation of the fit from the data below 2.1 eV demonstrates that the actual field-induced absorption onset is sharper than the one calculated from the model.

The shoulder appearing in the data at 2.35 eV may be associated with a second lower-energy Raman-active mode. Using fluorescence excitation spectroscopy, McBranch *et al.*<sup>33</sup> have demonstrated the existence of two Raman-active modes in the photoluminescence spectrum of oriented MEH-PPV/PE, and have identified the lower-energy mode as arising from the vinyl group and the higher-energy mode as arising from the phenyl ring. In contrast to the field-induced absorption spectrum, where the higher-energy mode clearly dominates, the photoluminescence, and absorption spectra suggest a more equal weighting for the two modes.

In Fig. 4, we demonstrate the modifications imparted to the  $G$  to  ${}^k B_u$  line shape caused by the filtering effects of the  ${}^m A_g$  symmetry state. The figure demonstrates that the dominant  ${}^m A_g$  symmetry state is more strongly coupled to  ${}^k B_u$  states near the band edge. A Fourier analysis of the filtered line shape suggests that the dominant  ${}^m A_g$  symmetry state has an intermediate localization length, i.e.,  $\xi_m/\xi_k \approx 1.2$ .

The dot-dash line in Fig. 4 is the deconvolved line shape of the  ${}^m A_g$  state resonance in the field-induced absorption spectrum as determined from the relative contribution of  $c_{a_g}^{(3)} L_{a_g}^{(3)}(\omega)$  in Eq. (7). The linewidth and

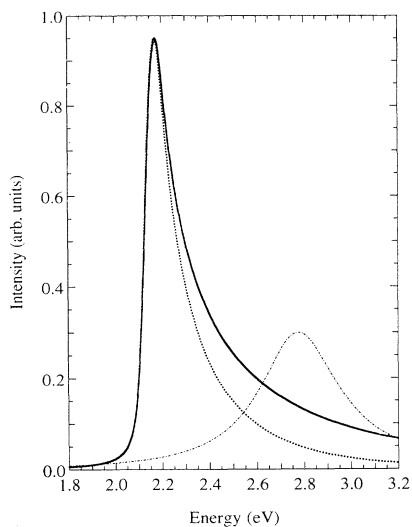


FIG. 4. The intrinsic line shape of the  $G$  to  ${}^k B_u$  transition as determined from the analysis of the electroabsorption spectrum (solid line) and the modified  $G$  to  ${}^k B_u$  line shape caused by the filtering effects of the  ${}^m A_g$  symmetry state (dashed line). A Fourier analysis of the filtered line shape suggests that the dominant  ${}^m A_g$  symmetry state has an intermediate localization length. Also shown is the deconvoluted line shape of the resonance in the field-induced absorption at 2.8 eV.

spectral position, with respect to the absorption onset, are consistent with the two-photon absorption spectrum of PPV.<sup>34</sup>

### C. Absorption vs electroabsorption

In Fig. 5, we compare the intrinsic line shape of the  $G$  to  ${}^k B_u$  transition as determined from the analysis of the absorption spectrum (dashed line) and the analysis of the electroabsorption spectrum (solid line). The line shapes have been corrected for the resolution of the spectrometer. Although there are slight differences between the  $G$  to  ${}^k B_u$  line shapes deconvoluted from the linear and nonlinear susceptibility, the results clearly demonstrate that the intrinsic line shape of the oriented, ordered MEH-PPV  $\pi$ -electron system is highly asymmetric, and can be modeled accurately in terms of a Gaussian broadened square-root singularity in the joint density of states.

Since the field-induced absorption is proportional to  $\chi^{(3)}(\omega, 0, 0)$  and  $\chi^{(3)}$  has been demonstrated both theoretically<sup>35–37</sup> and experimentally<sup>38–40</sup> to depend strongly on the localization length of the energy eigenstates, electroabsorption spectroscopy probes only the longest and most ordered conjugated segments in a given sample. In contrast, the linear susceptibility,  $\chi^{(1)}(\omega)$ , is primarily a function of the  $\pi$ -electron density, and is therefore, largely independent of the conjugation length. As a consequence, polarized absorption spectroscopy probes the entire conjugation length distribution, including the residual fraction of MEH-PPV in the polyethylene

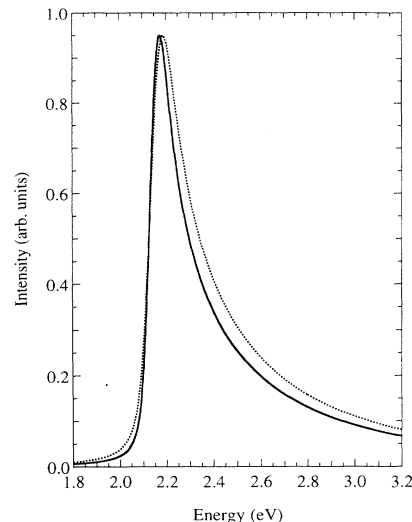


FIG. 5. The intrinsic line shape of the  $G$  to  ${}^k B_u$  transition as determined from the analysis of the absorption spectrum (dashed line) and the analysis of the electroabsorption spectrum (solid line). The results demonstrate that the intrinsic line shape of the oriented, ordered MEH-PPV  $\pi$ -electron system is highly asymmetric, and can be modeled accurately in terms of a Gaussian broadened square-root singularity in the joint density of states.

matrix, which has been demonstrated to be nonoriented and severely disordered.<sup>10</sup> Therefore, the discrepancy between the fitting parameters of the absorption spectrum and those of the electroabsorption spectrum is a quantitative measure of disorder.

The data presented in Table II and Fig. 4 indicate that the conjugation length distribution probed by EFM spectroscopy is essentially identical to that probed by linear absorption spectroscopy. This indicates that the conjugation length distribution function is well into the optical saturation regime, where both the energy gap and the ratio of  $\chi^{(3)}$  to  $\chi^{(1)}$  are independent of the conjugation length.<sup>36,37,39</sup> These results demonstrate that the linear and nonlinear optical properties of the oriented blend can be accurately described in terms of a single model with a limited number of parameters, and are not dominated by disorder or a distribution of conjugation lengths.

The most significant difference between the two measurements/analysis is the energy of the dominant Raman-active phonon mode, which is approximately 20 meV larger for the electroabsorption spectrum as compared to the absorption spectrum. The disparity in the phonon energies observed in the two measurements may provide

TABLE II. Analysis of  $A_g$  symmetry states in MEH-PPV/PE.

| Exp. | $E_m$ (eV) | $\Gamma_m$ (eV) | $\xi_m/\xi_k$ |
|------|------------|-----------------|---------------|
| EFM  | 2.77       | 0.10            | 1.2           |

insight into the nature of the dominant  ${}^m A_g$  symmetry state responsible for the field-induced absorption.

The matrix element probed by electroabsorption couples the ground state to the optically allowed  ${}^k B_u$  continuum, and the  ${}^k B_u$  continuum to the dominant  ${}^m A_g$  symmetry state, and is given by

$$\sum_k \int d^3 \mathbf{r} \psi_G^\dagger(\mathbf{r}) \mathbf{r} \psi_{k B_u}(\mathbf{r}) \times \left\{ \int_{\text{phenyl}} d^3 \mathbf{r}' \psi_{k B_u}^\dagger(\mathbf{r}') \mathbf{r}' \psi_{m A_g}(\mathbf{r}') + \int_{\text{vinylene}} d^3 \mathbf{r}' \psi_{k B_u}^\dagger(\mathbf{r}') \mathbf{r}' \psi_{m A_g}(\mathbf{r}') \right\}. \quad (12)$$

In writing Eq. (12), we have broken the matrix element involving the  ${}^m A_g$  symmetry state into an integral over the phenyl rings and an integral over the vinylene linkages. Because the unit cell in PPV contains eight  $\pi$  electrons, to a first approximation, the sum over  $k$  should be replaced by a sum over the momentum vectors of four nearly degenerate bands; three where the wave function amplitude is predominantly localized on the phenyl ring and one where the wave function amplitude is predominantly localized on the vinylene linkage. Hence, if the dominant  ${}^m A_g$  state is predominantly localized on the phenyl rings,<sup>41</sup> the sum over  $k$  will be dominated by those wave functions  ${}^k B_u$ , which have large amplitude on the phenyl rings. As a result, the vibronic structure observed in the EFM spectrum will be dominated by Raman-active lattice modes associated with the phenyl rings. This may explain why the phonon energies observed in the electroabsorption spectrum are larger than those observed in the absorption and photoluminescence spectra.

#### IV. CONCLUSION

Using a model which is based on the continuum version of the SSH model, we have fit the absorption and electroabsorption spectra of tensile drawn MEH-PPV/PE to an accuracy within experimental uncertainty. The absorption and field-induced absorption line shapes are accurately modeled in terms of a Gaussian-broadened one-dimensional square-root singularity in the joint density of states, the characteristic signature of a one-dimensional band structure. Although one might argue that the line shape asymmetry observed for the oriented blend is a manifestation of disorder or a distribution of conjugation lengths, this interpretation is clearly inconsistent with the sharp absorption onset, well defined vibronic structure, and the large polarization anisotropy of the field-induced absorption and the photoluminescence.

Furthermore, in light of the well-known conjugation length dependence of the nonlinear response, the similarity of the line shape parameters obtained by fitting the absorption and field-induced absorption spectra of the oriented blend indicates that gel processing and tensile drawing has yielded a MEH-PPV conjugation length distribution that is strongly peaked in the optical saturation regime, where both the energy gap and the ratio of  $\chi^{(3)}$  to  $\chi^{(1)}$  are independent of the conjugation length. Taken together, the data demonstrate convincingly that the joint density of states of the oriented, ordered MEH-PPV  $\pi$ -electron system is asymmetric.

#### ACKNOWLEDGMENTS

This research was supported by a grant from the Jet Propulsion Laboratory. T. W. Hagler was partially supported by the United States Department of Energy. We thank D. McBranch and F. Long for providing us with their Raman and fluorescence excitation spectroscopy results, and D. McBranch and A. Redondo for important comments and discussions.

<sup>1</sup> R. J. Elliott, Phys. Rev. **108**, 1384 (1957).

<sup>2</sup> T. Ogawa and T. Takagahara, Phys. Rev. B **44**, 8138 (1991).

<sup>3</sup> W. P. Su, J. R. Schrieffer, and A. J. Heeger, Phys. Rev. Lett. **42**, 1698 (1979).

<sup>4</sup> T. Tokihiro and E. Hanamura, Phys. Rev. Lett. **71**, 1423 (1993).

<sup>5</sup> U. Rauscher, H. Bässler, D. D. C. Bradley, and M. Hennecke, Phys. Rev. B **42**, 9830 (1990).

<sup>6</sup> U. Lemmer, R. F. Mahrt, Y. Wada, A. Greiner, H. Bässler, and E. O. Göbel, Appl. Phys. Lett. **62**, 2827 (1993).

<sup>7</sup> R. Kersting, U. Lemmer, R. F. Mahrt, K. Leo, H. Kurz, H. Bässler, and E. O. Göbel, Phys. Rev. Lett. **70**, 3820 (1993).

<sup>8</sup> H. Bässler, M. Gailberger, R. F. Mahrt, J. M. Oberski, and G. Weiser, Synth. Met. **49-50**, 341 (1992).

<sup>9</sup> A. Horvath, H. Bässler, and G. Weiser, Phys. Status Solidi B **173**, 755 (1992).

<sup>10</sup> T. W. Hagler, K. Pakbaz, K. F. Voss, and A. J. Heeger, Phys. Rev. B **44**, 8652 (1991).

<sup>11</sup> T. W. Hagler, K. Pakbaz, and A. J. Heeger, Phys. Rev. B

**49**, 10 968 (1994).

<sup>12</sup> P. Uznanski, M. Kryszewski, and E. W. Thulstrup, Spectrochim. Acta **46**, 23 (1980).

<sup>13</sup> T. W. Hagler and A. J. Heeger, Phys. Rev. B **49**, 7313 (1994).

<sup>14</sup> H. Takayama, Y. R. Lin-Liu, and K. Maki, Phys. Rev. B **21**, 2388 (1980).

<sup>15</sup> S. A. Brazovskii and N. N. Kirova, Pis'ma Zh. Eksp. Teor. Fiz. **33**, 6 (1981) [JETP Lett. **33**, 4 (1981)].

<sup>16</sup> K. Fesser, A. R. Bishop, and D. K. Campbell, Phys. Rev. B **27**, 4804 (1983).

<sup>17</sup> B. J. Orr and J. F. Ward, Mol. Phys. **20**, 513 (1971).

<sup>18</sup> W. Franz, Z. Naturforsch. Teil A **13**, 484 (1958).

<sup>19</sup> L. V. Keldysh, Zh. Eksp. Teor. Fiz. **34**, 1138 (1958) [Sov. Phys. JETP **7**, 788 (1958)].

<sup>20</sup> D. E. Aspnes and J. E. Rowe, Phys. Rev. B **5**, 4022 (1972).

<sup>21</sup> R. A. Street, T. M. Searle, I. G. Austin, and R. S. Sussmann, J. Phys. C **7**, 1582 (1974).

<sup>22</sup> G. G. Roberts, B. S. Keating, and A. V. Shelley, J. Phys. C **7**, 1595 (1974).

<sup>23</sup> S. Al Jalali and G. Weiser, J. Non-Cryst. Solids **41**, 1

- (1980).
- <sup>24</sup> G. Weiser, U. Dersch, and P. Thomas, *Philos. Mag. B* **57**, 721 (1988).
- <sup>25</sup> G. Weiser, *J. Non-Cryst. Solids* **114**, 250 (1989).
- <sup>26</sup> B. Esser, *Phys. Status Solidi* **51**, 735 (1972).
- <sup>27</sup> B. Esser and P. Kleinert, *Phys. Status Solidi* **68**, 265 (1975).
- <sup>28</sup> H. Overhof and K. Maschke, *J. Phys. Condens. Matter* **1**, 431 (1989).
- <sup>29</sup> H. Okamoto, K. Hattori, and Y. Hamakawa, *J. Non-Cryst. Solids* **137**, 627 (1991).
- <sup>30</sup> T. W. Hagler, *Chem. Phys. Lett.* **218**, 195 (1994).
- <sup>31</sup> G. Weiser, *Phys. Rev. B* **45**, 14 076 (1992).
- <sup>32</sup> B. Henderson and G. F. Imbusch, *Optical Spectroscopy of Inorganic Solids* (Clarendon Press, Oxford, 1989).
- <sup>33</sup> D. McBranch, F. Long, T. W. Hagler, K. Pakbaz, and A. J. Heeger, *Chem. Phys. Lett.* (to be published).
- <sup>34</sup> U. Lemmer, R. Fischer, J. Feldmann, R. F. Mahrt, J. Yang, A. Greiner, H. Bässler, and E. O. Göbel, *Chem. Phys. Lett.* **203**, 28 (1993).
- <sup>35</sup> K. C. Rustagi and J. Ducuing, *Opt. Commun.* **10**, 258 (1974).
- <sup>36</sup> Z. Shuai and J. L. Bredas, *Phys. Rev. B* **44**, 5962 (1991).
- <sup>37</sup> Z. Shuai and J. L. Bredas, *Phys. Rev. B* **46**, 4395 (1992).
- <sup>38</sup> J. P. Hermann and J. Ducuing, *J. Appl. Phys.* **45**, 5100 (1974).
- <sup>39</sup> H. Thienpont, G. L. J. A. Rikken, E. W. Meijer, W. ten Hoeve, and H. Wynberg, *Phys. Rev. Lett.* **65**, 2141 (1990).
- <sup>40</sup> L. T. Cheng, W. Tam, S. R. Marder, A. E. Stiegman, G. Rikken, and C. W. Spangler, *J. Phys. Chem.* **95**, 10 643 (1991).
- <sup>41</sup> Z. G. Soos, S. Ramasesha, D. S. Galvao, R. G. Kepler, and S. Etemad, *Synth. Met.* **54**, 35 (1993).